AMERICAN SOCIETY FOR MICROBIOLOGY | Applied and Environmental Microbiology®

MICROBIAL ECOLOGY

# Organohalide-Respiring Bacteria at the Heart of Anaerobic Metabolism in Arctic Wet Tundra Soils

David A. Lipson,[a] Theodore K. Raab,[b] Sherlynette Pérez Castro,[a]* Alexander Powell[a]

[a]Department of Biology, San Diego State University, San Diego, California, USA
[b]Department of Plant Biology, Carnegie Institution for Science, Stanford, California, USA

**ABSTRACT** Recent work revealed an active biological chlorine cycle in coastal Arctic tundra of northern Alaska. This raised the question of whether chlorine cycling was restricted to coastal areas or if these processes extended to inland tundra. The anaerobic process of organohalide respiration, carried out by specialized bacteria like *Dehalococcoides*, consumes hydrogen gas and acetate using halogenated organic compounds as terminal electron acceptors, potentially competing with methanogens that produce the greenhouse gas methane. We measured microbial community composition and soil chemistry along an ~262-km coastal-inland transect to test for the potential of organohalide respiration across the Arctic Coastal Plain and studied the microbial community associated with *Dehalococcoides* to explore the ecology of this group and its potential to impact C cycling in the Arctic. Concentrations of brominated organic compounds declined sharply with distance from the coast, but the decrease in organic chlorine pools was more subtle. The relative abundances of *Dehalococcoides* were similar across the transect, except for being lower at the most inland site. *Dehalococcoides* correlated with other strictly anaerobic genera, plus some facultative ones, that had the genetic potential to provide essential resources (hydrogen, acetate, corrinoids, or organic chlorine). This community included iron reducers, sulfate reducers, syntrophic bacteria, acetogens, and methanogens, some of which might also compete with *Dehalococcoides* for hydrogen and acetate. Throughout the Arctic Coastal Plain, *Dehalococcoides* is associated with the dominant anaerobes that control fluxes of hydrogen, acetate, methane, and carbon dioxide. Depending on seasonal electron acceptor availability, organohalide-respiring bacteria could impact carbon cycling in Arctic wet tundra soils.

**IMPORTANCE** Once considered relevant only in contaminated sites, it is now recognized that biological chlorine cycling is widespread in natural environments. However, linkages between chlorine cycling and other ecosystem processes are not well established. Species in the genus *Dehalococcoides* are highly specialized, using hydrogen, acetate, vitamin $B_{12}$-like compounds, and organic chlorine produced by the surrounding community. We studied which neighbors might produce these essential resources for *Dehalococcoides* species. We found that *Dehalococcoides* species are ubiquitous across the Arctic Coastal Plain and are closely associated with a network of microbes that produce or consume hydrogen or acetate, including the most abundant anaerobic bacteria and methanogenic archaea. We also found organic chlorine and microbes that can produce these compounds throughout the study area. Therefore, *Dehalococcoides* could control the balance between carbon dioxide and methane (a more potent greenhouse gas) when suitable organic chlorine compounds are available to drive hydrogen and acetate uptake.

**KEYWORDS** Arctic, *Dehalococcoides*, chlorine, methanogenesis, soil

Previous work revealed an active biological chlorine (Cl) cycle in coastal Arctic tundra, including *Dehalococcoides* species that use chlorinated organic ($Cl_{org}$) compounds as terminal electron ($e^-$) acceptors (TEAs) in anaerobic respiration (1).

**Citation** Lipson DA, Raab TK, Pérez Castro S, Powell A. 2021. Organohalide-respiring bacteria at the heart of anaerobic metabolism in Arctic wet tundra soils. Appl Environ Microbiol 87:e01643-20. https://doi.org/10.1128/AEM.01643-20.

**Editor** Knut Rudi, Norwegian University of Life Sciences



Address correspondence to David A. Lipson, dlipson@sdsu.edu.

* Present address: Sherlynette Pérez Castro, Ecosystem Center, Marine Biological Laboratory, Woods Hole, Massachusetts, USA.

**Received** 7 July 2020
**Accepted** 10 November 2020
**Accepted manuscript posted online** 13 November 2020
**Published** 15 January 2021

**TABLE 1** Sampling locations in the Arctic Coastal Plain, northern Alaska[a]

| Site | Latitude | Longitude | Distance to coast (km) | Elevation (m) |
|---|---|---|---|---|
| CST | 71.298 | −156.548 | 0.15–0.75 | 3 |
| 6km | 71.252 | −156.542 | 6 | 12 |
| 11k | 71.189 | −156.572 | 11 | 8 |
| 25k | 70.999 | −156.521 | 25 | 7 |
| ATQ | 70.470 | −157.408 | 48 | 17 |
| 100k | 70.069 | −156.106 | 110 | 37 |
| TFS | 68.624 | −149.585 | 192 | 730 |
| IVO | 68.480 | −155.758 | 262 | 582 |

[a]The four northernmost sites are near Utqiaġvik (Barrow). Distance to the coast is measured to the Beaufort Sea (or Elson Lagoon). ATQ, Atqasuk; TFS, Toolik Field Station; IVO, Ivotuk.

*Dehalococcoides* species are obligate organohalide-respiring bacteria with a high affinity for hydrogen gas ($H_2$), whose activity could therefore limit the availability of $H_2$ for methanogenesis and other metabolic processes (2). While originally studied in the context of bioremediation, there is growing interest in how organohalide respiration (OHR) might function in natural ecosystems (3). *Dehalococcoides* species are highly specialized in their requirements for $H_2$ as an energy source, acetate as a carbon (C) source, and various forms of $Cl_{org}$ or organic bromine ($Br_{org}$) compounds as TEAs (4). They have small, streamlined genomes (~1.4 Mb) but carry multiple reductive dehalogenase genes to utilize a wide variety of halogenated TEAs (5). *Dehalococcoides* species also require an exogenous supply of corrinoid building blocks to produce cobalamin (vitamin $B_{12}$), relying on the surrounding microbial community to provide these resources (6).

Being among the simplest biological energy sources, $H_2$ and acetate are central currencies for anaerobic metabolism, powering methanogenesis, iron (Fe) reduction, sulfate reduction, OHR, and autotrophic acetogenesis (in the case of $H_2$). The prevalence of *Dehalococcoides* in the microbial community of an Arctic wet tundra soil raised the question of how these important anaerobic pathways interact and whether OHR might serve as an important sink for $H_2$ and acetate that could otherwise fuel the production of methane ($CH_4$), a potent greenhouse gas. Previous work showed that saturated peat soils near Utqiaġvik (formerly Barrow), AK, host a broad diversity of anaerobic microbes and alternative TEA pathways (7–9). The experimental addition of ferric iron [Fe(III)] and humic acids to soils reduced $CH_4$ flux from soils (10), and another study demonstrated anaerobic oxidation of methane (AOM) in this ecosystem (11). These studies showed that the net flux of $CH_4$ from this ecosystem could be controlled by the presence of alternative TEAs. However, it is uncertain how *Dehalococcoides* and OHR fit into this network of supply and demand for $e^-$ donors and acceptors.

The discovery of significant biological Cl cycling in coastal tundra also raised the question of whether Cl cycling is restricted to coastal areas with high precipitation inputs of chloride ($Cl^-$) or whether OHR is a general feature of wet tundra soils. To address these questions, we conducted a survey of shotgun metagenomes and soil chemistry in wet tundra sites across the Arctic Coastal Plain (ACP) of northern Alaska from the coast of the Arctic Ocean to ~260 km inland (Table 1). We use the metagenomics data to identify which microbes are spatially associated with *Dehalococcoides* and have the genetic potential to provide or compete for essential resources.

## RESULTS

As expected, $Cl^-$ concentrations in snow and rain declined with distance from the coast (Fig. 1). Soil $Cl^-$ also declined sharply at distances of >25 km from the coast, although the progression was less regular than that for precipitation, implying local effects of hydrology and biology (Fig. 2). The soil concentrations of $Cl_{org}$ tended to decline with distance from the coast, although this trend was not significant [$P = 0.195$ for regression of $Cl_{org}$ versus ln(distance)]. Unlike Cl, total bromine (Br) was dominated by $Br_{org}$ across all sites, and $Br_{org}$ declined more dramatically with distance from the

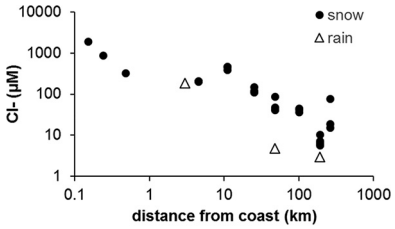


**FIG 1** Chloride concentrations in precipitation at sites along a coastal-inland transect starting near the Beaufort Sea.

coast than did $Cl_{org}$, with average $Br_{org}$ concentrations of the four most distant sites being 18% of that of the four coastal sites [$P = 0.004$ for regression of $Br_{org}$ versus ln(distance)].

Pools of soluble TEAs were generally dominated by Fe(III) (Fig. 3), with the exception of higher sulfate concentrations at the most coastal site (CST) and comparable Fe (III) and sulfate concentrations at the southernmost site (Ivotuk [IVO]). Nitrate concentrations were generally an order of magnitude lower than those of Fe(III) but were significantly higher at the two southernmost locations (Toolik Field Station [TFS] and IVO) than at the other sites ($P = 0.001$ by analysis of variance [ANOVA] with repeating contrast codes for relative position along transect). Acid-extractable Fe was abundant across all sites, although a significantly higher proportion was in the oxidized Fe(III) form in the two southernmost (and most topographically complex) sites ($P = 0.001$).

Averaging across all depths, the soil water concentrations of acetate ranged from 74 $\mu$M at IVO to 397 $\mu$M at CST, while the formate concentrations ranged from 22 $\mu$M at IVO to 140 $\mu$M at Atqasuk (ATQ). By two-way ANOVA, soil concentrations of acetate ($P = 0.008$) and formate ($P = 0.001$) differed significantly by site (driven mainly by lower concentrations at IVO), while the formate concentration was also significantly higher ($P = 0.006$) in deeper soil layers (Fig. 4).

The taxonomic structure of the microbial community was primarily driven by redox status and pH, and IVO clearly stood out from the other sites (Fig. 5). In the nonmetric multidimensional scaling (NMDS) analysis based on taxonomic groupings (phyla, except with *Proteobacteria*, which were broken into separate classes), surface soils (5 to 10 cm deep) were mainly distributed in the upper left diagonal of the plot, clearly separated from the deepest soil layer (circles versus diamonds in Fig. 5A to C). The taxo-

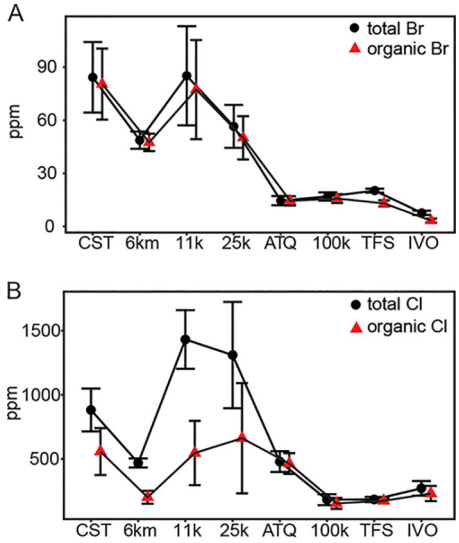


**FIG 2** Total and organic halogens (bromine [A] and chlorine [B]) in soils from the eight study locations, arranged from most coastal on the left to furthest inland on the right. In regressions on the log-transformed distance from the coast, $Br_{org}$ declined significantly ($P = 0.004$), while $Cl_{org}$ did not ($P = 0.195$).

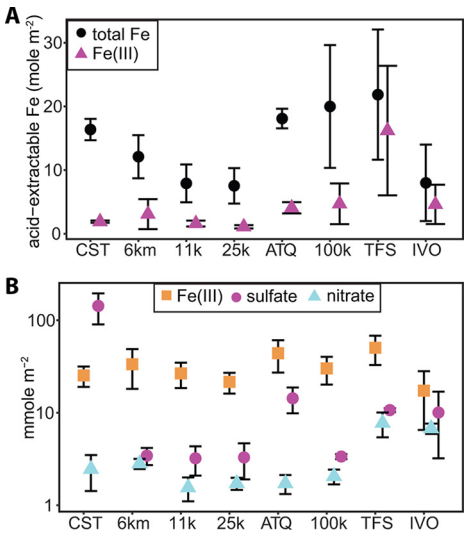


**FIG 3** Acid-extractable Fe (A) and soluble $e^-$ acceptors (B) from sites along the coastal-inland transect, integrated over a 35-cm soil profile. The nitrate concentrations and ratios of Fe(III)/total Fe were significantly higher at IVO and TFS ($P = 0.001$).

nomic structures differed among the three depths according to permutational multivariate analysis of variance (PerMANOVA) ($P < 0.01$ for all pairwise comparisons) (Fig. 5B). IVO stood out from the other sites, with both shallow (5 to 10 cm) and deeper (20 to 25 cm) samples appearing in the upper left of the plot (Fig. 5A). Taxonomically, IVO was distinct from the other sites by PerMANOVA ($P < 0.02$ for all pairwise comparisons) (Fig. 5A). In this analysis, TFS was also distinct from 11k ($P = 0.035$). The overlaid environmental vectors in Fig. 5C (using EnvFit) show that the taxonomic structure was driven by the redox status of soil Fe pools, pH, and concentrations of Fe(II), nitrate, and formate. These vectors show that IVO and the shallower soil layers were more oxic,

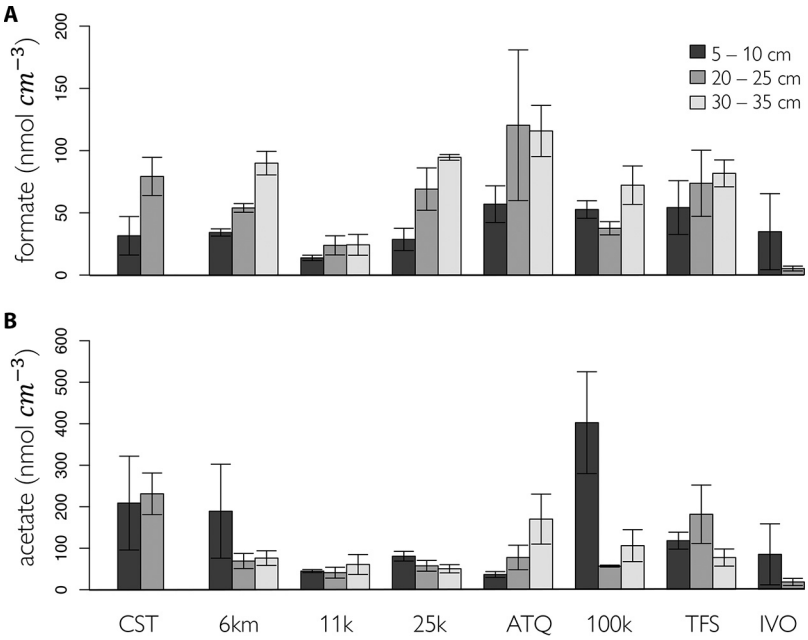


**FIG 4** Concentrations of formate (A) and acetate (B) in soils by depth and location along the coastal-inland transect. Soil concentrations of acetate ($P = 0.008$) and formate ($P = 0.001$) differed significantly by site, while the concentration of formate was also significantly higher ($P = 0.006$) in deeper soil layers.

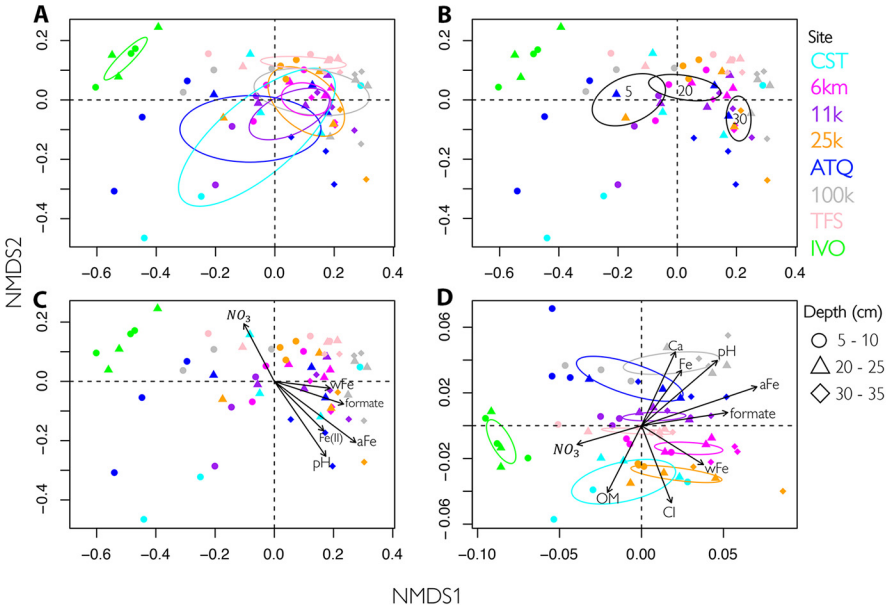


**FIG 5** Nonmetric multidimensional scaling (NMDS) analysis of 64 soil metagenomes showing samples by depth (symbols) and location (color). Data in panels A to C are based on taxonomic data (at the phylum level except for *Proteobacteria*, which were separated by class [stress = 0.092]), and data in panel D are based on functional data (SEED subsystem level 2 [stress = 0.17]). The 95% confidence ellipses around the centroids for each group are drawn for location (A and D) and depth (B). Taxonomically, IVO is significantly different from the other sites, and all 3 depths are different from each other. Functionally, all sites and depths differ significantly. Significant environmental variables are overlaid on taxonomic (C) and functional gene (D) ordinations. Ca, Cl, Fe, Fe(II), formate, $NO_3$, and $SO_4$ represent concentrations of these chemical species on a soil volume basis, while wFe and aFe are the ratios of Fe(II) to total Fe for water- and acid-extractable pools, respectively.

with higher concentrations of nitrate, while the other sites and deeper soil layers were more reduced, with higher concentrations of formate. Formate is interconvertible with $H_2$ by the enzyme formate hydrogen lyase (12) and is used interchangeably with $H_2$ by many anaerobes (13). The phylum-level composition of IVO was similar to those of the shallow samples from other sites, containing a higher abundance of phyla rich in aerobic and facultative species, such as *Acidobacteria* and *Alphaproteobacteria*, and fewer phyla with strict anaerobes, such as *Firmicutes* and *Euryarchaeota* (see Fig. S1 and S2 in the supplemental material).

Similarly, the NMDS based on metabolic pathways (SEED subsystem level 2) separated shallow samples from the deepest ones and placed IVO samples apart from those from the other sites (Fig. 5D). By PerMANOVAs of functional gene abundances, all pairwise comparisons of sites ($P < 0.002$) and depths ($P < 0.017$) were significant. According to the EnvFit analysis, the functional structure was driven by the same variables as those driven by the taxonomic structure, but chloride, calcium, and soil organic matter (SOM) contents were also significant (Fig. 5D).

IVO also stood out from the other sites in terms of the relative abundances of indicator taxa for strictly anaerobic processes: Fe reducers, sulfate reducers, OHR bacteria, syntrophic bacteria, and methanogens were comparably abundant at all sites except IVO, which was depleted of these groups (Fig. 6). By two-way ANOVA, the effects of site were highly significant for all indicator taxa ($P < 0.001$), and depth was significant for all indicators ($P < 0.05$) except *Geobacter* ($P = 0.233$).

*Dehalococcoides* and the closely related OHR genus *Dehalogenimonas* ($r = 0.989$) were ubiquitous in metagenomes across the ACP, and the relative abundance of this genus was highly correlated with a set of strict anaerobes as well as some facultative microbes (Fig. 7). The relative abundances of these genera according to Kaiju and MG-RAST were highly correlated (median Pearson $r = 0.95$), although one notable

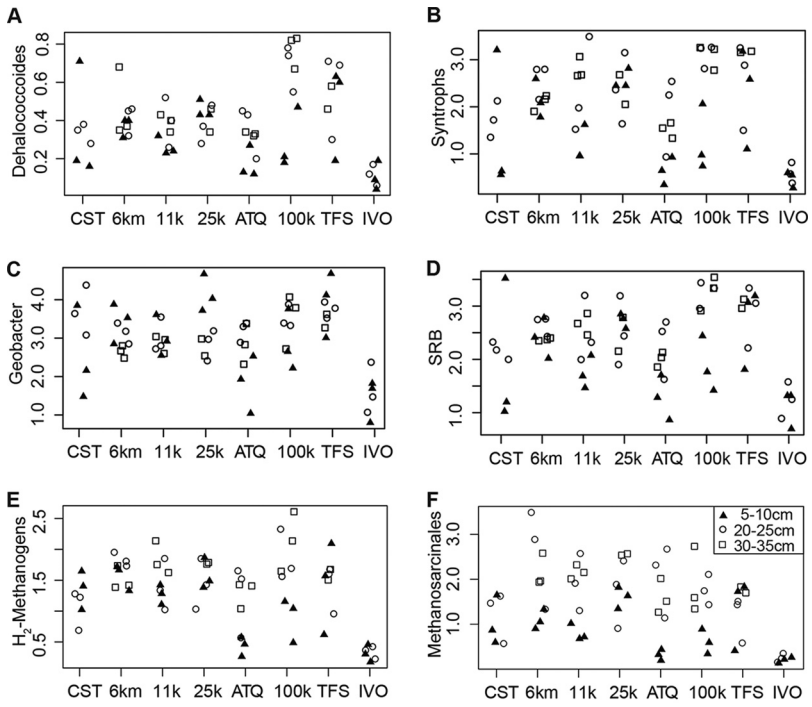


**FIG 6** Relative abundance (percent) of indicator taxa for anaerobic processes by depth and location along the transect. The effects of site were significant for all indicator taxa ($P < 0.001$), and depth was significant for all indicators ($P < 0.05$) except *Geobacter* ($P = 0.233$). SRB, sulfate-reducing bacteria.

difference between these annotations was that *Anaerolinea* was abundant by Kaiju but not detected by MG-RAST. Searches of assembled contigs with phmmer supported the presence of *Anaerolinea*, so this genus is included with *Chloroflexus* for the purposes of this study.

To explore the metabolic interdependence of this microbial network, the genera responsible for pathways that produce $H_2$, acetate, corrinoids, and $Cl_{org}$ were identified. Apart from aerobic and facultative bacteria with very different spatial distributions, *Dehalococcoides* was strongly associated with major producers of these essential resources (Fig. 7; see also Data Set S1 in the supplemental material). In addition to providing resources for *Dehalococcoides*, many of these microbes could also compete for resources, depending on the availability of $e^-$ acceptors (Fig. 8). Overall, the abundance of the genera shown in Fig. 7 was best predicted by the redox state of the acid-extractable Fe pool, soil pH, and formate concentration (Table 2), with a few notable exceptions, as discussed below.

## DISCUSSION

Our analysis reveals a network of potential interactions in which resources may be provided to *Dehalococcoides* when $Cl_{org}$ availability is high, directing $e^-$ flow away from $CH_4$ and toward $CO_2$ production. In addition to the commonly known syntrophic bacteria *Syntrophus* and *Synthrophobacter*, in the absence of alternative TEAs, other *Deltaproteobacteria* such as *Geobacter*, *Pelobacter*, and *Desulfovibrio* can also form syntrophic relationships in which $e^-$ is transferred to methanogens or other partners via $H_2$, formate, or direct interspecies electron transfer (DIET) (14–16). Given the high correlations of these genera with *Dehalococcoides* and the high affinity of *Dehalococcoides* for $H_2$ uptake, it is likely that *Dehalococcoides* species are viable alternative partners for syntrophic metabolism when suitable $Cl_{org}$ is available. This has been shown to be the case for a consortium of *Pelobacter* and *Dehalococcoides* species capable of degrading acetylene and trichloroethylene (17).

In addition to syntrophic bacteria, a variety of fermentative bacteria (*Bacteroidetes*,

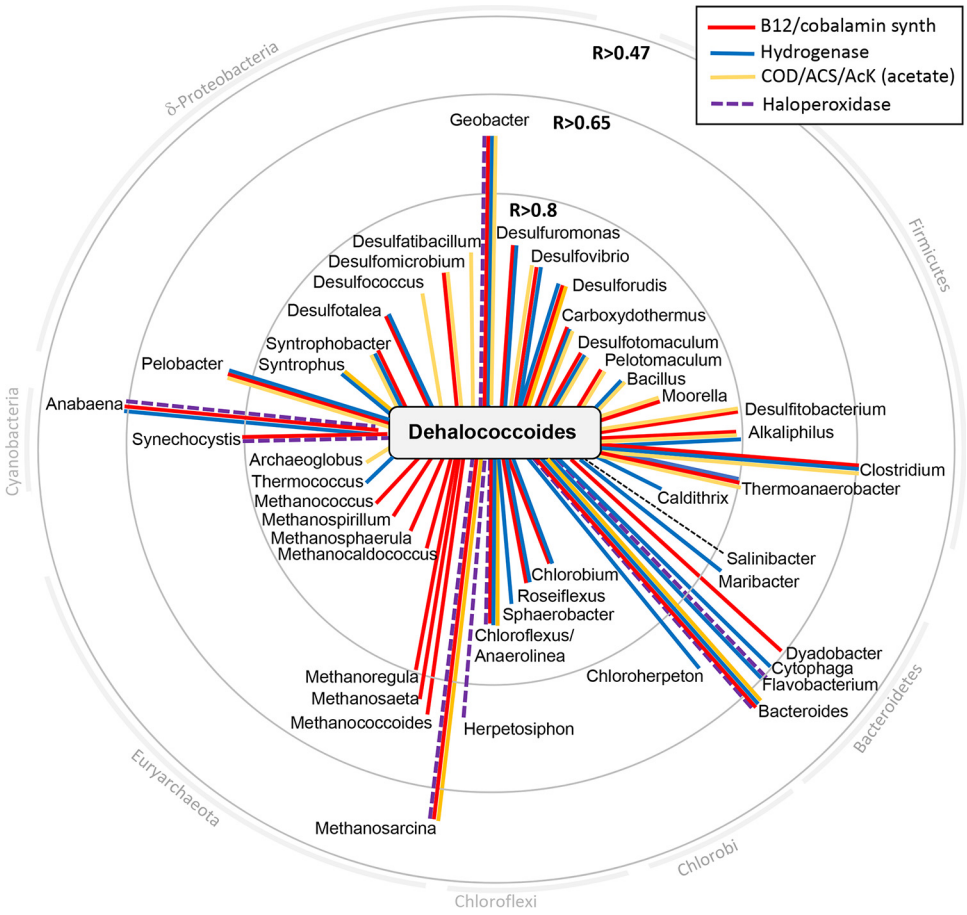


**FIG 7** Network of genera associated with *Dehalococcoides* and their potential to provide essential resources. Genera are arranged axially according to their correlation (*R*) with *Dehalococcoides*, with stronger correlations grouped toward the center, and radially according to phyla (note that *Caldithrix* is the sole representative of its phylum). Colored lines indicate the genetic potential of each to provide an essential resource to *Dehalococcoides*. See the text regarding possible $Cl_{org}$ synthesis by *Salinibacter*. Genera below ~0.1% abundance are not shown. COD, carbon monoxide dehydrogenase; ACS, acetyl CoA synthase; AcK, acetate kinase.

*Firmicutes*, and *Chloroflexi*) could provide $H_2$ through proton reduction or release formate and/or $H_2$ during mixed-acid fermentation. In fact, *Bacteroidetes* and other species not generally known for syntrophy have been implicated in the syntrophic transfer of $H_2$ in peat soil (18). Formate is readily converted to $H_2$ by formate hydrogen lyase, an enzyme found in many of the genomes represented in Fig. 7. *Dehalococcoides* species cannot grow using formate as the sole $e^-$ donor in pure culture (4) but are fueled by formate in enrichment cultures (19). Anoxygenic phototrophic bacteria, such as the green sulfur bacteria *Chlorobium* and *Chloroherpeton*, produce $H_2$ during photosynthesis and/or N fixation (20), and those capable of organotrophy in the dark (*Chloroflexus* and *Roseiflexus*) also fermentatively produce $H_2$ (21). The chemoautotroph *Carboxydothermus* produces $H_2$ and $CO_2$ from carbon monoxide. Most described species of *Maribacter* are aerobic, but several facultative species are known (22, 23), and the genome of *Maribacter cobaltidurans* has a hydrogenase gene very similar to a metagenomic sequence in this study. The *Maribacter* sequences identified in the current study appear to be from anaerobic species, as their abundance is positively correlated with the redox state of Fe and the concentration of formate, showing the same pattern as those of many of the well-known strict anaerobes (Table 2).

Acetogens (e.g., *Clostridium*, *Moorella*, *Thermoanaerobacter*, and *Archaeoglobus*) are potential donors of acetate (24, 25). While *Desulfitobacterium* species are capable of producing acetate (26), they also perform OHR (27), so the correlation with *Dehalococcoides*

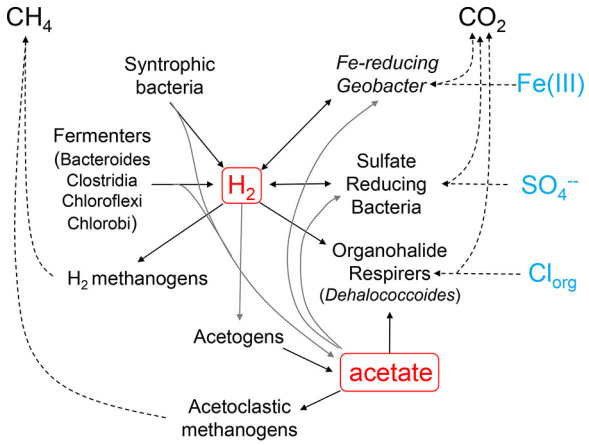


**FIG 8** Potential interactions among the functional groups shown in Fig. 7 with respect to $H_2$ and acetate cycling and the production of $CO_2$ and $CH_4$. Double-sided arrows for Fe and sulfate reducers show that $H_2$ can be produced or consumed, depending on the availability of terminal $e^-$ acceptors (shown in blue).

could arise from occupying a similar niche. Surprisingly, *Methanosarcina acetivorans* produces acetate when grown on carbon monoxide (28) but probably acts as a net consumer of acetate, overall. The presence of acetate kinase (AcK) genes linked to *Geobacter* and *Bacteroides* genomes indicates that mixed-acid fermentation is another potential source of acetate in this food web.

Many of the microbes shown in Fig. 7 have genes in cobalamin/vitamin $B_{12}$ synthesis pathways that are complementary to the incomplete set found in *Dehalococcoides* spp. and could potentially provide corrinoids for *Dehalococcoides*. For example, *Desulfovibrio vulgaris* provided $H_2$ and acetate, while *Pelosinus fermentans* provided corrinoids and acetate in a consortium with *Dehalococcoides mcartyi* (6), and *Geobacter lovleyi* provided corrinoids for the growth of *D. mcartyi* strain BAV1 (79). Several of the associated methanogenic genera are potential donors of corrinoids despite also being potential competitors for $H_2$ or acetate. These results are consistent with a metagenomic study of a *Dehalococcoides*-containing enrichment culture that also identified methanogens, *Deltaproteobacteria*, and *Firmicutes* as potential providers of corrinoids and other resources (29).

The precise source and chemical nature of $Cl_{org}$ in these soils remain a mystery, and it is uncertain what fraction of the total $Cl_{org}$ is suitable for OHR. Soil $Cl_{org}$ is complex, contains both labile and recalcitrant fractions, and can derive from both plants and microbes (30–32). In contrast to studies in forest soils, where the majority of $Cl_{org}$ is synthesized by the microbial chlorination of decomposing plant litter (33, 34), Arctic mosses and sedges appear to be significant initial sources of $Cl_{org}$ (1). Despite this, the same study found diverse microbial haloperoxidase (HPO) genes in Arctic soil metagenomes, and $Cl_{org}$ in older peats became more chemically complex, indicating that SOM is reworked by cycles of microbial dehalogenation and halogenation over time. The full diversity of HPOs in these microbial communities is beyond the scope of the present study, but a diverse set of HPOs belong to taxa that are highly correlated with *Dehalococcoides*. Cyanobacteria living in dark, anoxic soil layers would be a surprising source of $Cl_{org}$ for OHR. Despite generally living as photoautotrophs, many cyanobacteria, including species of *Anabaena*, are capable of fermentation (35). *Synechocystis* is a metabolically flexible genus capable of at least aerobic growth on glucose (36). In addition to their ability to grow heterotrophically in the dark, both genera are motile, which may also help explain their presence throughout the soil profile. One likely function for HPO enzymes is to protect against oxidative stress (37). Reactive oxygen species (ROS) are generated during photosynthesis, and cyanobacteria have been implicated in the production of halogenated organic compounds in marine environments (38). In strict anaerobes like *Anaerolinea*, *Bacteroides*, *Geobacter*, and

**TABLE 2** Pearson correlation coefficients of the relative abundances of genera shown in Fig. 7 with soil chemical variables and *Dehalococcoides* abundance

| Genus | *r* value[a] | | | |
|---|---|---|---|---|
| | Acid-extractable $Fe^{2+}$/total Fe | Formate (nmol $cm^{-3}$) | pH | *Dehalococcoides* |
| *Dehalococcoides* | **0.442** | **0.351** | **0.331** | **1** |
| *Dehalogenimonas* | **0.449** | 0.276 | 0.313 | **0.989** |
| *Desulforudis* | **0.441** | **0.334** | **0.337** | **0.924** |
| *Desulfococcus* | **0.471** | **0.329** | 0.316 | **0.917** |
| *Thermococcus* | **0.466** | 0.310 | **0.392** | **0.917** |
| *Desulfotalea* | **0.501** | **0.376** | **0.345** | **0.909** |
| *Desulfovibrio* | **0.369** | 0.275 | 0.263 | **0.908** |
| *Desulfatibacillum* | **0.447** | 0.311 | 0.266 | **0.904** |
| *Desulfuromonas* | **0.388** | 0.284 | **0.350** | **0.903** |
| *Moorella* | **0.505** | **0.381** | **0.376** | **0.896** |
| *Carboxydothermus* | **0.513** | **0.379** | **0.394** | **0.891** |
| *Caldithrix* | 0.313 | 0.191 | 0.116 | **0.885** |
| *Syntrophobacter* | 0.217 | 0.194 | 0.209 | **0.874** |
| *Pelotomaculum* | **0.506** | **0.359** | **0.462** | **0.863** |
| *Methanocaldococcus* | **0.456** | 0.289 | **0.335** | **0.861** |
| *Methanospirillum* | **0.497** | **0.373** | **0.351** | **0.849** |
| *Methanococcus* | **0.565** | **0.398** | **0.376** | **0.843** |
| *Archaeoglobus* | **0.457** | 0.316 | 0.318 | **0.841** |
| *Bacillus* | **0.525** | **0.473** | **0.412** | **0.835** |
| *Desulfotomaculum* | **0.556** | **0.434** | **0.377** | **0.831** |
| *Syntrophus* | **0.535** | 0.301 | 0.252 | **0.830** |
| *Roseiflexus* | 0.212 | 0.200 | 0.315 | **0.825** |
| *Desulfomicrobium* | **0.521** | 0.318 | **0.345** | **0.822** |
| *Chlorobium* | **0.570** | **0.461** | 0.318 | **0.811** |
| *Chloroflexus* | 0.175 | 0.181 | 0.314 | **0.804** |
| *Methanosphaerula* | **0.515** | **0.336** | **0.346** | **0.804** |
| *Sphaerobacter* | 0.303 | 0.200 | **0.409** | **0.801** |
| *Thermoanaerobacter* | **0.539** | **0.417** | **0.405** | **0.798** |
| *Methanocorpusculum* | **0.509** | **0.387** | **0.402** | **0.788** |
| *Herpetosiphon* | 0.163 | 0.186 | 0.288 | **0.781** |
| *Methanoregula* | **0.434** | 0.304 | 0.270 | **0.780** |
| *Chloroherpeton* | **0.391** | **0.355** | 0.193 | **0.772** |
| *Salinibacter* | 0.203 | 0.132 | 0.128 | **0.759** |
| *Methanosaeta* | **0.349** | 0.134 | 0.226 | **0.752** |
| *Methanococcoides* | **0.515** | **0.341** | **0.402** | **0.737** |
| *Desulfitobacterium* | **0.56** | **0.475** | **0.429** | **0.724** |
| *Pelobacter* | **0.404** | **0.339** | **0.415** | **0.715** |
| *Synechocystis* | 0.123 | 0.171 | 0.059 | **0.699** |
| *Geobacter* | 0.279 | 0.196 | **0.371** | **0.685** |
| *Maribacter* | **0.579** | **0.359** | **0.348** | **0.666** |
| *Alkaliphilus* | **0.558** | **0.482** | **0.402** | **0.651** |
| *Dyadobacter* | **0.565** | **0.415** | 0.303 | **0.602** |
| *Spirosoma* | **0.528** | **0.403** | 0.212 | **0.587** |
| *Flavobacterium* | **0.598** | **0.455** | **0.335** | **0.504** |
| *Cytophaga* | **0.573** | **0.446** | 0.291 | **0.497** |
| *Anabaena* | −0.117 | 0.057 | −0.110 | **0.493** |
| *Clostridium* | **0.533** | **0.515** | **0.350** | **0.476** |
| *Methanosarcina* | **0.522** | **0.415** | 0.260 | **0.473** |
| *Bacteroides* | **0.569** | **0.464** | **0.336** | **0.471** |

[a]Correlations significant at a *P* value of <0.001 are shown in boldface type, those significant at a *P* value of <0.05 are shown in regular typeface, and those with a *P* value of >0.05 are shaded ($n = 64$).

*Methanosarcina*, ROS could also arise due to Fenton chemistry from the active Fe cycle that occurs in these ecosystems (39). Specific natural halogenated products may also serve antagonistic roles (40, 41). However, given the promiscuous substrate affinities of most HPOs, it has been questioned whether they are the enzymes responsible for the synthesis of most specific natural products (42; but see reference 43). While cyanobacteria are known to produce halogenated compounds with

antagonistic or toxic properties (44, 45), such compounds have rarely, if ever, been found in strictly anaerobic organisms (42), so the HPO genes associated with the genomes of *Anaerolinea*, *Bacteroides*, *Geobacter*, and *Methanosarcina* are more likely to play a role in oxidative stress.

Most of the microbes whose abundance was highly correlated with that of *Dehalococcoides* require anoxic environments and either produce or consume $H_2$ or acetate. The more surprising associations are those with facultative microbes, particularly cyanobacteria and *Salinibacter*. From Table 2 and published descriptions of their physiology, it is clear that the correlation of these organisms with *Dehalococcoides* does not arise from having similar habitat requirements. *Salinibacter ruber* is reported to be aerobic (46), although its genome has a full set of genes for fermentation pathways and microaerobic growth (47). As discussed above, *Anabaena* and *Synechocystis* could provide $Cl_{org}$ for OHR. The genome of *S. ruber* contains a gene annotated as an *S*-adenosyl-L-methionine (SAM)-dependent chlorinase/fluorinase. This gene is highly related to chlorinase and fluorinase genes found in *Salinispora tropica* and other bacteria (48). It is not certain that this annotation is correct, as other genes in this family are actually hydrolases with little or no halogenase activity (49). However, a metabolomics study of this species revealed a number of halogenated compounds (80; Josefa Antón, personal communication). The presence of a putative chlorinase gene and halogenated metabolites in *Salinibacter* and the otherwise unexpected association of these two very different bacteria raise the possibility that *Dehalococcoides* benefits from $Cl_{org}$ provided by *Salinibacter*. In a previous survey across a broad range of ecosystems, the abundance of *Dehalococcoides* was correlated with the ratio of $Cl_{org}$/total organic C in soil (50).

The anaerobic metabolic network in these Arctic wet tundra soils is highly interconnected and flexible. Species of *Geobacter* and *Desulfovibrio* could switch from their preferred TEAs to syntrophic partnerships with methanogens or OHR bacteria when labile $Cl_{org}$ is present. It is also likely that anaerobic methane-oxidizing *Euryarchaeota* (ANME) perform anaerobic oxidation of methane (AOM) independently or in consortia with bacterial reducers of Fe(III), sulfate, and maybe even $Cl_{org}$. AOM has been demonstrated in Alaskan coastal Arctic tundra, possibly coupled to Fe(III) reduction (11). Using shotgun metagenomic data, it is not generally practical to differentiate between species within the same genus. Most ANME are taxonomically distinct from methanogenic *Archaea*, although *M. acetivorans* can both produce and oxidize methane (51). Furthermore, *Methanosarcina* is phylogenetically related to ANME groups 3 and 2a/b (52). Therefore, the sequences assigned to *Methanosarcina* may include ANME. AOM consortia with OHR bacteria have not yet been described, although their existence is possible given that ANME can transfer $e^-$ to bacterial partners through DIET or possibly acetate (51, 53, 54). The lack of genetic evidence for $H_2$ formation in ANME (51) and the lack of cytochromes in *Dehalococcoides* that could receive $e^-$ through DIET (5) argue against this possibility. However, *Methanosarcina* strains produce $H_2$ during acetoclastic methanogenesis (55), so it is plausible that this genus and related *Archaea* could provide $H_2$ to *Dehalococcoides* rather than solely acting as competitors for energetic molecules.

The correlations among microbial genera found among the 64 metagenomes of this study imply spatial colocalization but not necessarily simultaneous activity. It is likely that $H_2$ is partitioned between different groups of anaerobically respiring bacteria and methanogens depending on the seasonal availability of TEAs. $Cl_{org}$ compounds used in OHR have reduction potentials comparable to those of nitrate (56) and theoretically should be used preferentially before Fe(III) or sulfate. However, other factors may prevent OHR from attaining the maximum theoretical energy yield from these reactions (57), and published $H_2$ threshold values for OHR are in the range of ~0.2 to 2.5 nM, overlapping those of Fe(III) and sulfate reduction but still well below the concentrations required for methanogenesis (2, 58, 59). Both solid-phase and dissolved Fe become increasingly reduced throughout the summer in soils near Utqiaġvik (9). Meanwhile, methanogenesis proceeds throughout the summer (60), probably due to

high concentrations of acetate (Fig. 4). By late summer or fall, the general exhaustion of TEA pools might allow hydrogenotrophic methanogens to thrive, as indicated by a shift from acetoclastic to hydrogenotrophic methanogenesis between July and September (61). Future studies of the seasonal dynamics of these functional groups will be necessary to understand the true ecological implications of the correlations demonstrated here.

In summary, the anaerobic microbial community of wet tundra soils is a complex web of syntrophy and commensalism, with *Dehalococcoides* as an integral and highly connected component, even in sites up to 200 km from the coast. While *Dehalococcoides* generally accounts for less than 1% of metagenomic sequences (the small genome of ~1.4 Mb notwithstanding), given their high capacity for $H_2$ oxidation and their intimate associations with so many key players in the Arctic C cycle, there may be times in the season when they control the flow of anaerobic metabolism.

## MATERIALS AND METHODS

**Sampling locations and methodology.** The eight study locations extend from the northern coast of Alaska near Utqiaġvik (Barrow) to the southern edge of the Arctic Coastal Plain near the foothills of the Brooks Range (Table 1). The sites were chosen to increase in distance logarithmically away from the coast and to represent wet tundra dominated by mosses and graminoids (62). The area sampled in Ivotuk is characterized as moist acidic tundra (63) but includes wet areas with a high water table dominated by sphagnum mosses and sedges (64). In April 2018, three replicate soil cores were collected from each site using a gas-powered drill and a 7.5-cm-diameter SIPRE auger corer (Jon's Machine Shop, Fairbanks, AK). Most cores reached depths of 35 cm or more, although some were shallower (depending on the state of the soil and auger teeth). Frozen soil samples were placed in vacuum seal bags in a cooler, immediately vacuum sealed upon return from the field, and remained at −40°C until transport to San Diego, CA.

Snow was collected near the time of maximum accumulation, in April 2008. Snow depth was measured above each soil core, and samples were collected with an acrylonitrile butadiene styrene (ABS) cylinder and transferred to Saranex ziplock bags (Bitran; Fisher Scientific). Samples were weighed to determine density and water content. Rain was collected opportunistically in July 2018 at Utqiaġvik, Atqasuk, and TFS by leaving a polyethylene box in the landscape during a single rain event at each of these three locations. Rain samples were transferred to polypropylene vials and frozen for later analysis.

**Precipitation and soil chemistry.** Frozen soil cores were cut into horizontal sections with a band saw, measured, and weighed. Each horizon was subdivided longitudinally, and subsamples were used for gravimetric water content (dried to a constant weight at 105°C), organic matter content (loss on combustion at 500°C overnight), water and acid extractions, or DNA extractions (stored at −80°C). For extractions, slices of frozen soil (~5 to 10 g) were placed into preweighed vials of 25 ml $N_2$-degassed ultrapure $H_2O$ or 1 N $H_2SO_4$, reweighed, and shaken for 1 h, and aliquots were removed and centrifuged at high speed to remove soil. Water extracts were analyzed by ion chromatography, and a separate aliquot was acidified with a drop of $H_2SO_4$ to preserve the samples for Fe analysis. Inorganic and small organic anions were measured in soil water extracts and precipitation samples by ion chromatography (Dionex ICS5000$^+$). Fe(II) and total Fe in water and acid extracts were measured using 1,10-phenanthroline (8). Cations were measured by ion-coupled plasma optical emission spectroscopy (ICP-OES) on 1% nitric acid extracts of ash from combusted soils.

**Metagenomic sequencing and analysis.** Soil DNA was extracted using Qiagen MoBio PowerSoil kits, quantified using a Qubit fluorometer, and sent to the University of California—Davis DNA Technologies Core facility for library construction and Illumina HiSeq 4000 PE150 shotgun sequencing. Barcode-indexed sequencing libraries were generated from genomic DNA samples sheared on an E220 focused ultrasonicator (Covaris, Woburn, MA). For each sample, 50 ng sheared DNA was converted to sequencing libraries using a Kapa HyperPrep library kit (catalog number KK8504; Kapa Biosystems-Roche, Basel, Switzerland). The libraries were amplified with 11 PCR cycles, analyzed with a Bioanalyzer 2100 instrument (Agilent, Santa Clara, CA), quantified by fluorometry on a Qubit instrument (Life Technologies, Carlsbad, CA), and combined in two pools at equimolar ratios. The pools were quantified by quantitative PCR (qPCR) with a Kapa Library Quant kit (Kapa Biosystems-Roche), and each pool was sequenced on one lane of an Illumina HiSeq 4000 instrument (Illumina, San Diego, CA) with paired-end 150-bp reads. The pre-quality-control (QC) metagenomes averaged 427 Mb in length (standard deviation, 59 Mb). Post-QC metagenomes averaged 345 ± 46 Mbp, with 1.25 million ± 0.17 million sequences averaging 275 ± 0.7 bp in length. Details for individual metagenomes are shown in Table S1 in the supplemental material.

We based our initial assignments of taxonomy and function for metagenomic data on the MG-RAST pipeline version 4.0 (81, 82). In this pipeline, data are trimmed to remove low-quality reads and dereplicated to remove artificial duplicate reads, and protein-coding genes are identified using FragGeneScan, clustered into similarity groups, and identified using DIAMOND against the M5nr database, which integrates the GenBank, SEED IMG, UniProt, KEGG, and EGGNOG databases.

We used PerMANOVA to compare taxonomic and functional gene abundances across metagenomes. Bray-Curtis dissimilarities between relative sequence abundance profiles were compared using the adonis

function of the vegan package (65). When significant effects were found, multiple comparisons were performed using the pairwise.perm.manova function within the RVAideMemoire package (66). The EnvFit function was used to overlay significant environmental variables on the NMDS ordination using the metaMDS function in the vegan package, and component scores were used to generate 95% confidence ellipses around centroids using the ordiellipse() function within vegan.

To identify microbes that might provide *Dehalococcoides* with essential resources, we searched the SEED subsystems for cobalamin synthesis, vitamin $B_{12}$ synthesis, acetogenesis, HPO, and hydrogenases. The genera responsible for the majority of annotations of these genes were initially selected for correlation analysis to quantify their cooccurrence with *Dehalococcoides*. As an independent confirmation of the taxonomic profiles generated in MG-RAST, the relative abundances of genera (the number of hits for a genus divided by the total number of hits in a metagenome) were compared with the output from Kaiju in KBase (67). The functional roles of these genera were verified as described below (see also Data Set S2 in the supplemental material), and additions or subtractions were made as new evidence was gathered.

To confirm the ability of the identified genera to provide useful corrinoid cofactors, we searched the annotated metagenomes and public genomes in SEED (68) or KBase (67) for vitamin $B_{12}$ or cobalamin synthesis genes that were complementary to those found in *Dehalococcoides* (which, according to SEED, include CbiA, CobA, CbiP, CobD, CbiB, CobU, CobT, CobC, and CobS). To infer acetogenesis in a genus, we verified the presence of carbon monoxide dehydrogenase and acetyl-CoA synthase in the metagenomes, or published genomes from the same genus, and literature reports of acetate production by members of the genus, when available. The presence of these genes in methanogens was assumed to indicate acetate uptake rather than production, although *M. acetivorans* produces acetate when grown on carbon monoxide (28). To include the possibility of acetate production through mixed-acid fermentation, we used HMMER (69) to perform a hidden Markov model (HMM) search on assembled metagenomes for acetate kinase, using an HMM profile built from the alignment for Pfam domain PF00871 (70), and identified the most likely genomic source for these genes using phmmer searches against the UniProt database.

Initially, we searched MG-RAST for Fe hydrogenase (EC 1.6.5.3), an enzyme likely to be involved in the syntrophic transfer of $H_2$ (71). However, this search in MG-RAST also identified many respiratory complex I genes belonging to probable aerobes. To produce a more definitive list of microbes capable of producing $H_2$ and/or formate, we assembled a subset of the metagenomes using MetaSPades (assembly details are provided in Table S2 in the supplemental material) and annotated them using Prokka within the KBase platform. Genes for Ni-Fe and Fe-Fe hydrogenases and formate hydrogen lyase were identified (72), and phmmer was used to search the UniProt database for their most likely taxonomic source (73). The presence of hydrogenases in publicly available genomes and literature reports of $H_2$ production provided supplemental evidence (Data Set S2).

The SEED annotation in MG-RAST identified HPO genes in only a few genera. However, a more thorough search of the assembled genomes revealed a great diversity of HPOs, the full results of which are beyond the scope of the current study, which is restricted to just those taxa that are highly correlated with *Dehalococcoides*. A subset of metagenomes was assembled using MetaSPades in KBase. The resulting contigs were downloaded, and predicted proteins were found using Prodigal (74). The proteins were searched with HMMER (69) using HMM profiles generated from MUSCLE protein alignments (75) for nonmetal and vanadium-dependent HPO (VHPO) genes available from Pfam (70). Authentic HPO genes were differentiated from related gene families by aligning the putative HPO sequences with curated HPO genes and other hydrolase genes in the case of nonmetal HPO (76, 77) or acid phosphatase genes in the case of VHPO (78). We also assembled draft genomes from our metagenomes in KBase: contigs were binned with MaxBin2, quality checked with CheckM, annotated with RAST, and classified using SpeciesTree, GTDB-Tk Classify, and BLASTp searches with ribosomal proteins. Metagenome-assembled genomes (MAGs) with a completeness of at least 50% and contamination of less than 10% were searched using the HMM profiles for HPO described above. A description of these MAGs and references to the identified genomic features are presented in Table S3 in the supplemental material.

**Data availability.** These metagenomes are publicly available on the MG-RAST server as project mgp87497 (www.mg-rast.org/mgmain.html?mgpage=project&project=mgp87497). The MAGs used to verify the presence of HPO genes in certain genera are available in KBase as a narrative entitled "HPO-MAGs" (https://narrative.kbase.us/narrative/73786).

## SUPPLEMENTAL MATERIAL

Supplemental material is available online only.

**SUPPLEMENTAL FILE 1**, PDF file, 0.4 MB.

**SUPPLEMENTAL FILE 2**, XLSX file, 0.03 MB.

**SUPPLEMENTAL FILE 3**, XLSX file, 0.05 MB.

## ACKNOWLEDGMENTS

We thank CPS and UIC for invaluable logistical assistance and Josefa Antón for generously sharing metabolomics data.

Sequencing was carried out at the DNA Technologies and Expression Analysis Cores at the UC Davis Genome Center, supported by NIH shared instrumentation grant 1S10OD010786-01. This work was funded by NSF grant 1712774 to D.A.L.

## REFERENCES


1. Zlamal JE, Raab TK, Little M, Edwards RA, Lipson DA. 2017. Biological chlorine cycling in the Arctic Coastal Plain. Biogeochemistry 134:243–260. https://doi.org/10.1007/s10533-017-0359-0.
2. Löffler FE, Tiedje JM, Sanford RA. 1999. Fraction of electrons consumed in electron acceptor reduction and hydrogen thresholds as indicators of halorespiratory physiology. Appl Environ Microbiol 65:4049–4056. https://doi.org/10.1128/AEM.65.9.4049-4056.1999.
3. Atashgahi S, Häggblom MM, Smidt H. 2018. Organohalide respiration in pristine environments: implications for the natural halogen cycle. Environ Microbiol 20:934–948. https://doi.org/10.1111/1462-2920.14016.
4. Löffler FE, Yan J, Ritalahti KM, Adrian L, Edwards EA, Konstantinidis KT, Müller JA, Fullerton H, Zinder SH, Spormann AM. 2013. Dehalococcoides mccartyi gen. nov., sp. nov., obligately organohalide-respiring anaerobic bacteria relevant to halogen cycling and bioremediation, belong to a novel bacterial class, Dehalococcoidia classis nov., order Dehalococcoidales ord. nov. and family Dehalococcoidaceae fam. nov., within the phylum Chloroflexi. Int J Syst Evol Microbiol 63:625–635. https://doi.org/10.1099/ijs.0.034926-0.
5. Kube M, Beck A, Zinder SH, Kuhl H, Reinhardt R, Adrian L. 2005. Genome sequence of the chlorinated compound-respiring bacterium Dehalococcoides species strain CBDB1. Nat Biotechnol 23:1269–1273. https://doi.org/10.1038/nbt1131.
6. Men Y, Seth EC, Yi S, Allen RH, Taga ME, Alvarez-Cohen L. 2014. Sustainable growth of Dehalococcoides mccartyi 195 by corrinoid salvaging and remodeling in defined lactate-fermenting consortia. Appl Environ Microbiol 80:2133–2141. https://doi.org/10.1128/AEM.03477-13.
7. Lipson DA, Haggerty JM, Srinivas A, Raab TK, Sathe S, Dinsdale EA. 2013. Metagenomic insights into anaerobic metabolism along an Arctic peat soil profile. PLoS One 8:e64659. https://doi.org/10.1371/journal.pone.0064659.
8. Lipson DA, Jha M, Raab TK, Oechel WC. 2010. Reduction of iron (III) and humic substances plays a major role in anaerobic respiration in an Arctic peat soil. J Geophys Res 115:G00I06. https://doi.org/10.1029/2009JG001147.
9. Lipson DA, Raab TK, Goria D, Zlamal J. 2013. The contribution of Fe(III) and humic acid reduction to ecosystem respiration in drained thaw lake basins of the Arctic Coastal Plain. Global Biogeochem Cycles 27:399–409. https://doi.org/10.1002/gbc.20038.
10. Miller KE, Lai C-T, Friedman ES, Angenent LT, Lipson DA. 2015. Methane suppression by iron and humic acids in soils of the Arctic Coastal Plain. Soil Biol Biochem 83:176–183. https://doi.org/10.1016/j.soilbio.2015.01.022.
11. Miller KE, Lai C-T, Dahlgren RA, Lipson DA. 2019. Anaerobic methane oxidation in high-arctic Alaskan peatlands as a significant control on net CH4 fluxes. Soil Syst 3:7. https://doi.org/10.3390/soilsystems3010007.
12. McDowall JS, Murphy BJ, Haumann M, Palmer T, Armstrong FA, Sargent F. 2014. Bacterial formate hydrogenlyase complex. Proc Natl Acad Sci U S A 111:E3948–E3956. https://doi.org/10.1073/pnas.1407927111.
13. Ferry JG. 1990. Formate dehydrogenase. FEMS Microbiol Rev 7:377–382. https://doi.org/10.1111/j.1574-6968.1990.tb04940.x.
14. Li X, McInerney MJ, Stahl DA, Krumholz LR. 2011. Metabolism of H2 by Desulfovibrio alaskensis G20 during syntrophic growth on lactate. Microbiology 157:2912–2921. https://doi.org/10.1099/mic.0.051284-0.
15. Rotaru A-E, Shrestha PM, Liu F, Markovaite B, Chen S, Nevin K, Lovley D. 2014. Direct interspecies electron transfer between Geobacter metallireducens and Methanosarcina barkeri. Appl Environ Microbiol 80:4599–4605. https://doi.org/10.1128/AEM.00895-14.
16. Sieber JR, McInerney MJ, Gunsalus RP. 2012. Genomic insights into syntrophy: the paradigm for anaerobic metabolic cooperation. Annu Rev Microbiol 66:429–452. https://doi.org/10.1146/annurev-micro-090110-102844.
17. Mao X, Oremland RS, Liu T, Gushgari S, Landers AA, Baesman SM, Alvarez-Cohen L. 2017. Acetylene fuels TCE reductive dechlorination by defined Dehalococcoides/Pelobacter consortia. Environ Sci Technol 51:2366–2372. https://doi.org/10.1021/acs.est.6b05770.
18. Schmidt O, Hink L, Horn MA, Drake HL. 2016. Peat: home to novel syntrophic species that feed acetate- and hydrogen-scavenging methanogens. ISME J 10:1954–1966. https://doi.org/10.1038/ismej.2015.256.
19. Mayer-Blackwell K, Azizian MF, Green JK, Spormann AM, Semprini L. 2017. Survival of vinyl chloride respiring Dehalococcoides mccartyi under long-term electron donor limitation. Environ Sci Technol 51:1635–1642. https://doi.org/10.1021/acs.est.6b05050.
20. Warthmann R, Pfennig N, Cypionka H. 1993. The quantum requirement for H2 production by anoxygenic phototrophic bacteria. Appl Microbiol Biotechnol 39:358–362. https://doi.org/10.1007/BF00192092.
21. Kondratieva EN, Ivanovsky RN, Krasilnikova EN. 1992. Carbon metabolism in Chloroflexus aurantiacus. FEMS Microbiol Lett 100:269–271. https://doi.org/10.1111/j.1574-6968.1992.tb05714.x.
22. Hu J, Yang Q-Q, Ren Y, Zhang W-W, Zheng G, Sun C, Pan J, Zhu X-F, Zhang X-Q, Wu M. 2015. Maribacter thermophilus sp. nov., isolated from an algal bloom in an intertidal zone, and emended description of the genus Maribacter. Int J Syst Evol Microbiol 65:36–41. https://doi.org/10.1099/ijs.0.064774-0.
23. Zhang GI, Hwang CY, Kang S-H, Cho BC. 2009. Maribacter antarcticus sp. nov., a psychrophilic bacterium isolated from a culture of the Antarctic green alga Pyramimonas gelidicola. Int J Syst Evol Microbiol 59:1455–1459. https://doi.org/10.1099/ijs.0.006056-0.
24. Ragsdale SW, Pierce E. 2008. Acetogenesis and the Wood-Ljungdahl pathway of CO2 fixation. Biochim Biophys Acta 1784:1873–1898. https://doi.org/10.1016/j.bbapap.2008.08.012.
25. Labes A, Schönheit P. 2001. Sugar utilization in the hyperthermophilic, sulfate-reducing archaeon Archaeoglobus fulgidus strain 7324: starch degradation to acetate and CO2 via a modified Embden-Meyerhof pathway and acetyl-CoA synthetase (ADP-forming). Arch Microbiol 176:329–338. https://doi.org/10.1007/s002030100330.
26. Kreher S, Schilhabel A, Diekert G. 2008. Enzymes involved in the anoxic utilization of phenyl methyl ethers by Desulfitobacterium hafniense DCB2 and Desulfitobacterium hafniense PCE-S. Arch Microbiol 190:489–495. https://doi.org/10.1007/s00203-008-0400-8.
27. Nonaka H, Keresztes G, Shinoda Y, Ikenaga Y, Abe M, Naito K, Inatomi K, Furukawa K, Inui M, Yukawa H. 2006. Complete genome sequence of the dehalorespiring bacterium Desulfitobacterium hafniense Y51 and comparison with Dehalococcoides ethenogenes 195. J Bacteriol 188:2262–2274. https://doi.org/10.1128/JB.188.6.2262-2274.2006.
28. Rother M, Metcalf WW. 2004. Anaerobic growth of Methanosarcina acetivorans C2A on carbon monoxide: an unusual way of life for a methanogenic archaeon. Proc Natl Acad Sci U S A 101:16929–16934. https://doi.org/10.1073/pnas.0407486101.
29. Hug LA, Beiko RG, Rowe AR, Richardson RE, Edwards EA. 2012. Comparative metagenomics of three Dehalococcoides-containing enrichment cultures: the role of the non-dechlorinating community. BMC Genomics 13:327. https://doi.org/10.1186/1471-2164-13-327.
30. Montelius M, Svensson T, Lourino-Cabana B, Thiry Y, Bastviken D. 2016. Chlorination and dechlorination rates in a forest soil—a combined modelling and experimental approach. Sci Total Environ 554–555:203–210. https://doi.org/10.1016/j.scitotenv.2016.02.208.
31. Öberg G, Bastviken D. 2012. Transformation of chloride to organic chlorine in terrestrial environments: variability, extent, and implications. Crit Rev Environ Sci Technol 42:2526–2545. https://doi.org/10.1080/10643389.2011.592753.
32. Leri AC, Myneni SCB. 2010. Organochlorine turnover in forest ecosystems: the missing link in the terrestrial chlorine cycle. Global Biogeochem Cycles 24:GB4021. https://doi.org/10.1029/2010GB003882.
33. Öberg G, Nordlund E, Berg B. 1996. In situ formation of organically bound halogens during decomposition of Norway spruce needles: effects of fertilization. Can J For Res 26:1040–1048. https://doi.org/10.1139/x26-115.
34. Öberg G, Holm M, Sandén P, Svensson T, Parikka M. 2005. The role of organic-matter-bound chlorine in the chlorine cycle: a case study of the Stubbetorp catchment, Sweden. Biogeochemistry 75:241–269. https://doi.org/10.1007/s10533-004-7259-9.
35. Stal LJ, Moezelaar R. 1997. Fermentation in cyanobacteria. FEMS Microbiol Rev 21:179–211. https://doi.org/10.1016/S0168-6445(97)00056-9.
36. Tang K-H, Tang Y, Blankenship R. 2011. Carbon metabolic pathways in phototrophic bacteria and their broader evolutionary implications. Front Microbiol 2:165. https://doi.org/10.3389/fmicb.2011.00165.

37. Bengtson P, Bastviken D, Öberg G. 2013. Possible roles of reactive chlorine II: assessing biotic chlorination as a way for organisms to handle oxygen stress. Environ Microbiol 15:991–1000. https://doi.org/10.1111/j.1462-2920.2012.02807.x.
38. Karlsson A, Auer N, Schulz-Bull D, Abrahamsson K. 2008. Cyanobacterial blooms in the Baltic—a source of halocarbons. Mar Chem 110:129–139. https://doi.org/10.1016/j.marchem.2008.04.010.
39. Trusiak A, Treibergs LA, Kling GW, Cory RM. 2019. The controls of iron and oxygen on hydroxyl radical (·OH) production in soils. Soil Syst 3:1. https://doi.org/10.3390/soilsystems3010001.
40. Bengtson P, Bastviken D, De Boer W, Öberg G. 2009. Possible role of reactive chlorine in microbial antagonism and organic matter chlorination in terrestrial environments. Environ Microbiol 11:1330–1339. https://doi.org/10.1111/j.1462-2920.2009.01915.x.
41. van Pée K-H, Unversucht S. 2003. Biological dehalogenation and halogenation reactions. Chemosphere 52:299–312. https://doi.org/10.1016/S0045-6535(03)00204-2.
42. van Pée K-H, Dong C, Flecks S, Naismith J, Patallo EP, Wage T. 2006. Biological halogenation has moved far beyond haloperoxidases. Adv Appl Microbiol 59:127–157. https://doi.org/10.1016/S0065-2164(06)59005-7.
43. Bernhardt P, Okino T, Winter JM, Miyanaga A, Moore BS. 2011. A stereoselective vanadium-dependent chloroperoxidase in bacterial antibiotic biosynthesis. J Am Chem Soc 133:4268–4270. https://doi.org/10.1021/ja201088k.
44. Wright AD, Papendorf O, König GM. 2005. Ambigol C and 2,4-dichlorobenzoic acid, natural products produced by the terrestrial cyanobacterium Fischerella ambigua. J Nat Prod 68:459–461. https://doi.org/10.1021/np049640w.
45. Esquenazi E, Daly M, Bahrainwala T, Gerwick WH, Dorrestein PC. 2011. Ion mobility mass spectrometry enables the efficient detection and identification of halogenated natural products from cyanobacteria with minimal sample preparation. Bioorg Med Chem 19:6639–6644. https://doi.org/10.1016/j.bmc.2011.06.081.
46. Antón J, Oren A, Benlloch S, Rodríguez-Valera F, Amann R, Rosselló-Mora R. 2002. Salinibacter ruber gen. nov., sp. nov., a novel, extremely halophilic member of the Bacteria from saltern crystallizer ponds. Int J Syst Evol Microbiol 52:485–491. https://doi.org/10.1099/00207713-52-2-485.
47. Mongodin EF, Nelson KE, Daugherty S, Deboy RT, Wister J, Khouri H, Weidman J, Walsh DA, Papke RT, Sanchez Perez G, Sharma AK, Nesbø CL, MacLeod D, Bapteste E, Doolittle WF, Charlebois RL, Legault B, Rodriguez-Valera F. 2005. The genome of Salinibacter ruber: convergence and gene exchange among hyperhalophilic bacteria and archaea. Proc Natl Acad Sci U S A 102:18147–18152. https://doi.org/10.1073/pnas.0509073102.
48. Deng H, Botting CH, Hamilton JT, Russell RJ, O'Hagan D. 2008. S-Adenosyl-L-methionine:hydroxide adenosyltransferase: a SAM enzyme. Angew Chem Int Ed Engl 47:5357–5361. https://doi.org/10.1002/anie.200800794.
49. Eustáquio AS, Härle J, Noel JP, Moore BS. 2008. S-Adenosyl-L-methionine hydrolase (adenosine-forming), a conserved bacterial and archeal protein related to SAM-dependent halogenases. Chembiochem 9:2215–2219. https://doi.org/10.1002/cbic.200800341.
50. Krzmarzick MJ, Crary BB, Harding JJ, Oyerinde OO, Leri AC, Myneni SC, Novak PJ. 2012. Natural niche for organohalide-respiring Chloroflexi. Appl Environ Microbiol 78:393–401. https://doi.org/10.1128/AEM.06510-11.
51. McGlynn SE. 2017. Energy metabolism during anaerobic methane oxidation in ANME archaea. Microbes Environ 32:5–13. https://doi.org/10.1264/jsme2.ME16166.
52. Winkel M, Sepulveda-Jauregui A, Martinez-Cruz K, Heslop J, Rijkers R, Horn F, Liebner S, Anthony KW. 2019. First evidence for cold-adapted anaerobic oxidation of methane in deep sediments of thermokarst lakes. Environ Res Commun 1:e021002. https://doi.org/10.1088/2515-7620/ab1042.
53. Cai C, Shi Y, Guo J, Tyson GW, Hu S, Yuan Z. 2019. Acetate production from anaerobic oxidation of methane via intracellular storage compounds. Environ Sci Technol 53:7371–7379. https://doi.org/10.1021/acs.est.9b00077.
54. Wang F-P, Zhang Y, Chen Y, He Y, Qi J, Hinrichs K-U, Zhang X-X, Xiao X, Boon N. 2014. Methanotrophic archaea possessing diverging methane-oxidizing and electron-transporting pathways. ISME J 8:1069–1078. https://doi.org/10.1038/ismej.2013.212.
55. Zinder S, Anguish T. 1992. Carbon monoxide, hydrogen, and formate metabolism during methanogenesis from acetate by thermophilic cultures of Methanosarcina and Methanothrix strains. Appl Environ Microbiol 58:3323–3329. https://doi.org/10.1128/AEM.58.10.3323-3329.1992.
56. Atashgahi S, Liebensteiner MG, Janssen DB, Smidt H, Stams AJ, Sipkema D. 2018. Microbial synthesis and transformation of inorganic and organic chlorine compounds. Front Microbiol 9:3079. https://doi.org/10.3389/fmicb.2018.03079.
57. Schubert T, Adrian L, Sawers RG, Diekert G. 2018. Organohalide respiratory chains: composition, topology and key enzymes. FEMS Microbiol Ecol 94:fiy035. https://doi.org/10.1093/femsec/fiy035.
58. Yang Y, McCarty PL. 1998. Competition for hydrogen within a chlorinated solvent dehalogenating anaerobic mixed culture. Environ Sci Technol 32:3591–3597. https://doi.org/10.1021/es980363n.
59. Heimann A, Jakobsen R, Blodau C. 2010. Energetic constraints on H2-dependent terminal electron accepting processes in anoxic environments: a review of observations and model approaches. Environ Sci Technol 44:24–33. https://doi.org/10.1021/es9018207.
60. Zona D, Gioli B, Commane R, Lindaas J, Wofsy SC, Miller CE, Dinardo SJ, Dengel S, Sweeney C, Karion A, Chang RY-W, Henderson JM, Murphy PC, Goodrich JP, Moreaux V, Liljedahl A, Watts JD, Kimball JS, Lipson DA, Oechel WC. 2016. Cold season emissions dominate the Arctic tundra methane budget. Proc Natl Acad Sci U S A 113:40–45. https://doi.org/10.1073/pnas.1516017113.
61. Throckmorton HM, Heikoop JM, Newman BD, Altmann GL, Conrad MS, Muss JD, Perkins GB, Smith LJ, Torn MS, Wullschleger SD, Wilson CJ. 2015. Pathways and transformations of dissolved methane and dissolved inorganic carbon in Arctic tundra watersheds: evidence from analysis of stable isotopes. Global Biogeochem Cycles 29:1893–1910. https://doi.org/10.1002/2014GB005044.
62. US Fish and Wildlife Service. 2003. CAVM. Circumpolar Arctic vegetation map. Scale, 1:7,500,000. US Fish and Wildlife Service, Anchorage, AK.
63. Riedel SM, Epstein HE, Walker DA, Richardson DL, Calef MP, Edwards E, Moody A. 2005. Spatial and temporal heterogeneity of vegetation properties among four tundra plant communities at Ivotuk, Alaska, USA. Arct Antarct Alp Res 37:25–33. https://doi.org/10.1657/1523-0430(2005)037[0025:SATHOV]2.0.CO;2.
64. McEwing KR, Fisher JP, Zona D. 2015. Environmental and vegetation controls on the spatial variability of CH4 emission from wet-sedge and tussock tundra ecosystems in the Arctic. Plant Soil 388:37–52. https://doi.org/10.1007/s11104-014-2377-1.
65. Oksanen J, Blanchet F, Friendly M, Kindt R, Legendre P, McGlinn D, Minchin P, O'Hara R, Simpson G, Solymos P. 2019. vegan: community ecology package. R package version 2.5.4.
66. Hervé M. 2020. Package 'RVAideMemoire'. https://CRAN.R-project.org/package=RVAideMemoire.
67. Arkin AP, Cottingham RW, Henry CS, Harris NL, Stevens RL, Maslov S, Dehal P, Ware D, Perez F, Canon S, Sneddon MW, Henderson ML, Riehl WJ, Murphy-Olson D, Chan SY, Kamimura RT, Kumari S, Drake MM, Brettin TS, Glass EM, Chivian D, Gunter D, Weston DJ, Allen BH, Baumohl J, Best AA, Bowen B, Brenner SE, Bun CC, Chandonia J-M, Chia J-M, Colasanti R, Conrad N, Davis JJ, Davison BH, DeJongh M, Devoid S, Dietrich E, Dubchak I, Edirisinghe JN, Fang G, Faria JP, Frybarger PM, Gerlach W, Gerstein M, Greiner A, Gurtowski J, Haun HL, He F, Jain R, et al. 2018. KBase: the United States department of energy systems biology knowledgebase. Nat Biotechnol 36:566–569. https://doi.org/10.1038/nbt.4163.
68. Overbeek R, Begley T, Butler RM, Choudhuri JV, Chuang H-Y, Cohoon M, de Crécy-Lagard V, Diaz N, Disz T, Edwards R, Fonstein M, Frank ED, Gerdes S, Glass EM, Goesmann A, Hanson A, Iwata-Reuyl D, Jensen R, Jamshidi N, Krause L, Kubal M, Larsen N, Linke B, McHardy AC, Meyer F, Neuweger H, Olsen G, Olson R, Osterman A, Portnoy V, Pusch GD, Rodionov DA, Rückert C, Steiner J, Stevens R, Thiele I, Vassieva O, Ye Y, Zagnitko O, Vonstein V. 2005. The subsystems approach to genome annotation and its use in the project to annotate 1000 genomes. Nucleic Acids Res 33:5691–5702. https://doi.org/10.1093/nar/gki866.
69. Eddy SR. 2011. Accelerated profile HMM searches. PLoS Comput Biol 7:e1002195. https://doi.org/10.1371/journal.pcbi.1002195.
70. El-Gebali S, Mistry J, Bateman A, Eddy SR, Luciani A, Potter SC, Qureshi M, Richardson LJ, Salazar GA, Smart A, Sonnhammer ELL, Hirsh L, Paladin L, Piovesan D, Tosatto SCE, Finn RD. 2019. The Pfam protein families database in 2019. Nucleic Acids Res 47:D427–D432. https://doi.org/10.1093/nar/gky995.
71. Sieber JR, Sims DR, Han C, Kim E, Lykidis A, Lapidus AL, McDonnald E, Rohlin L, Culley DE, Gunsalus R, McInerney MJ. 2010. The genome of Syntrophomonas wolfei: new insights into syntrophic metabolism and biohydrogen production. Environ Microbiol 12:2289–2301. https://doi.org/10.1111/j.1462-2920.2010.02237.x.
72. Greening C, Biswas A, Carere CR, Jackson CJ, Taylor MC, Stott MB, Cook GM, Morales SE. 2016. Genomic and metagenomic surveys of hydrogenase

distribution indicate H2 is a widely utilised energy source for microbial growth and survival. ISME J 10:761–777. https://doi.org/10.1038/ismej.2015.153.
73. Potter SC, Luciani A, Eddy SR, Park Y, Lopez R, Finn RD. 2018. HMMER Web server: 2018 update. Nucleic Acids Res 46:W200–W204. https://doi.org/10.1093/nar/gky448.
74. Hyatt D, Chen G-L, LoCascio PF, Land ML, Larimer FW, Hauser LJ. 2010. Prodigal: prokaryotic gene recognition and translation initiation site identification. BMC Bioinformatics 11:119. https://doi.org/10.1186/1471-2105-11-119.
75. Edgar RC. 2004. MUSCLE: multiple sequence alignment with high accuracy and high throughput. Nucleic Acids Res 32:1792–1797. https://doi.org/10.1093/nar/gkh340.
76. Hofmann B, Tölzer S, Pelletier I, Altenbuchner J, Van Pee K, Hecht H. 1998. Structural investigation of the cofactor-free chloroperoxidases. J Mol Biol 279:889–900. https://doi.org/10.1006/jmbi.1998.1802.
77. Pelletier I, Altenbuchner J. 1995. A bacterial esterase is homologous with nonhaem haloperoxidases and displays brominating activity. Microbiology 141:459–468. https://doi.org/10.1099/13500872-141-2-459.
78. Littlechild J, Garcia-Rodriguez E, Dalby A, Isupov M. 2002. Structural and functional comparisons between vanadium haloperoxidase and acid phosphatase enzymes. J Mol Recognit 15:291–296. https://doi.org/10.1002/jmr.590.
79. Yan J, Ritalahti KM, Wagner DD, Löffler FE. 2012. Unexpected specificity of interspecies cobamide transfer from *Geobacter* spp. to organohalide-respiring *Dehalococcoides mccartyi* strains. Appl Environ Microbiol 78:6630–6636. https://doi.org/10.1128/aem.01535-12.
80. Antón J, Lucio M, Peña A, Cifuentes A, Brito-Echeverría J, Moritz F, Tziotis D, López C, Urdiain M, Schmitt-Kopplin P. 2013. High metabolomic microdiversity within co-occurring isolates of the extremely halophilic bacterium *Salinibacter ruber*. PLoS One 8:e64701. https://doi.org/10.1371/journal.pone.0064701.
81. Meyer F, Paarmann D, D'Souza M, Olson R, Glass EM, Kubal M, Paczian T, Rodriguez A, Stevens R, Wilke A, Wilkening J, Edwards RA. 2008. The metagenomics RAST server – a public resource for the automatic phylogenetic and functional analysis of metagenomes. BMC Bioinformatics 9:386. https://doi.org/10.1186/1471-2105-9-386.
82. Wilke A, Bischof J, Harrison T, Brettin T, D'Souza M, Gerlach W, Matthews H, Paczian T, Wilkening J, Glass EM. 2015. A RESTful API for accessing microbial community data for MG-RAST. PLoS Comp Biol 11:e1004008. https://doi.org/10.1371/journal.pcbi.1004008.